Tissue-equivalent materials for construction of tomographic dosimetry phantoms in pediatric radiology

A. K. Jones
Department of Nuclear and Radiological Engineering, University of Florida, Gainesville, Florida 32611-8300

D. E. Hintenlang and W. E. Bolch[a)]
Department of Nuclear and Radiological Engineering and Department of Biomedical Engineering, University of Florida, Gainesville, Florida 32611-8300

(Received 10 April 2003; revised 29 May 2003; accepted for publication 29 May 2003; published 23 July 2003)

Tissue equivalent materials have a variety of uses, including routine quality assurance and quality control in both diagnostic and therapeutic physics. They are frequently used in a research capacity to measure doses delivered to patients undergoing various therapeutic procedures. However, very few tissue equivalent materials have been developed for research use at the low photon energies encountered in diagnostic radiology. In this paper, we present a series of tissue-equivalent (TE) materials designed to radiographically mimic human tissue at diagnostic photon energies. These tissue equivalent materials include STES–NB (newborn soft tissue substitute), BTES–NB (newborn bone tissue substitute), LTES (newborn as well as a child/adult lung tissue substitute), STES (child/adult soft tissue substitute), and BTES (child/adult bone tissue substitute). In all cases, targeted reference elemental compositions are taken from those specified in the ORNL stylized computational model series. For each material, reference values of mass density, mass attenuation coefficients (10–150 keV), and mass energy-absorption coefficients (10–150 keV) were matched as closely as permitted by material selection and manufacturing constraints. Values of μ/ρ and μ_{en}/ρ for the newborn TE materials are noted to have maximum deviations from their ORNL reference values of from 0 to −3% and from +2% to −3%, respectively, over the diagnostic energy range 10–150 keV. For the child/adult TE materials, these same maximal deviations of μ/ρ and μ_{en}/ρ are from +1.5% to −3% and from +3% to −3%, respectively. Simple calculations of x-ray fluence attenuation under narrow-beam geometry using a 66 kVp spectrum typical of newborn CR radiographs indicate that the tissue-equivalent materials presented here yield estimates of absorbed dose at depth to within 3.6% for STES–NB, 3.2% for BTES–NB, and 1.2% for LTES of the doses assigned to reference newborn soft, bone, and lung tissue, respectively. [DOI: 10.1118/1.1592641]

Key words: tissue-equivalent material, muscle-equivalent, bone-equivalent, lung-equivalent, pediatric radiology, diagnostic physics

I. INTRODUCTION

The search for materials to represent human tissue has been ongoing since Keinböck in 1906 first proposed water as being muscle equivalent.[1] Since that time, refinements and new developments have occurred in tissue-equivalent (TE) materials for use in both diagnostic and therapeutic radiology.[2] These materials play a vital role in activities ranging from specialized dosimetry research to daily quality assurance and radiation treatment planning. While inexpensive and readily available materials such as acrylic and aluminum are suitable for quality assurance in diagnostic radiology, they may not be suitable for research dosimetry purposes, especially at the low energies (<120 keV) used in pediatric radiology. As part of our efforts to construct a series of pediatric computational models and physical phantoms based upon CT imaging data,[3] our research team has developed tissue-equivalent substitutes that are radiographically representative of the soft, skeletal, and lung tissues of the newborn patient. Further refinements to these materials have been made so that they represent these same tissues in older patients (1 year through the adult). Targeted reference tissue compositions for this work were taken as defined by Cristy and Eckerman for the Oak Ridge National Laboratory (ORNL) stylized model series.[4]

It is noted that more extensive and organ-specific reference elemental compositions have been published such as given in Publication 46 of the International Commission on Radiological Units and Measurements (ICRU).[5] However, methods of phantom construction at the University of Florida (UF) are based upon image segmentation and material differentiation of only the soft tissue, lung tissue, and skeletal tissue regions found in each tomographic image slice. As described previously by Sessions *et al.*[6] for our newborn stylized dosimetry phantom, internal dose estimates for soft tissue organs are determined via internal MOSFET dosimeter placement within regions constructed of average soft tissue-equivalent material. Furthermore, experimental uncertainties in MOSFET dosimetry would most likely make efforts to

 0094-2405/2003/30(8)/2072/10/$20.00

develop organ-specific (e.g., liver) soft tissue-equivalent substitutes unjustified.

All tissue substitutes developed at the UF are designed to be simple to manufacture, and to yield a rigid yet machineable plastic when cured. In the present study, comparisons are made to a variety of other materials currently used in quality assurance measurements and medical dosimetry studies. As a final demonstration of tissue-equivalency, calculations of simple exponential attenuation and single-collision absorbed dose at depth are performed at diagnostic energies under narrow-beam geometry for the UF TE substitutes, other TE materials in current use, and the ORNL reference tissues. The long-term objective of our studies is the construction of a physical tomographic model of the newborn following the CT image segmentation previously described by Nipper *et al.*[3]

II. MATERIALS AND METHODS

The tissue-equivalent materials discussed here are all manufactured with an epoxy resin base in which phenolic microspheres are used to adjust the mass density. A more complete discussion of epoxy resin systems, their use in tissue substitutes, as well as the use of phenolic microspheres in these tissue substitutes can be found in papers by White and his colleagues.[7,8] All bone-equivalent materials developed at UF are constructed to represent a homogeneous mixture of cortical and trabecular spongiosa (bone trabeculae and bone marrow). The material compositions of each tissue substitute were adjusted to closely match values of (1) mass density, (2) mass attenuation coefficients, and (3) mass energy-absorption coefficients for the proper ORNL reference tissues over the diagnostic photon energy range applicable to pediatric radiological examinations. The development process involved three steps. First iterative adjustments to White's original material compositions were made to match both the mass attenuation and mass energy-absorption coefficients of the ORNL reference tissues in the diagnostic energy range. Second, phenolic microspheres were then added to match the mass density of each ORNL reference tissue. Finally, fine adjustments to materials compositions were made to rematch interaction coefficients over the diagnostic energy range, while maintaining the correct mass density.

A. Soft tissue-equivalent substitute for the newborn (STES–NB)

The soft tissue-equivalent substitute STES–NB was developed to be radiographically equivalent to reference newborn soft tissue as defined by Cristy and Eckerman.[4] STES–NB is manufactured using a base of Araldite GY-6010, an epoxy resin, with Jeffamine T-403, a hardener. The proportions used are roughly similar to those originally proposed for use at therapeutic photon energies by White and colleagues,[7] but adjusted in our research for tissue equivalency at diagnostic energies. Filler materials include polyethylene, silicon dioxide, and magnesium oxide. Phenolic microspheres are also incorporated to produce the desired mass density.

B. Bone tissue-equivalent substitute for the newborn (BTES–NB)

A bone tissue-equivalent substitute BTES–NB was developed to be radiographically equivalent to reference homogeneous newborn skeletal tissue as defined by Cristy and Eckerman.[4] BTES–NB, like its soft-tissue counterpart STES–NB, is manufactured using a base of Araldite GY-6010 with a Jeffamine T-403 hardener, in proportions similar to those originally proposed by White and colleagues.[7] Filler materials for BTES–NB include polyvinyl chloride, silicon dioxide, and calcium carbonate added in proportions needed to match values of mass density, mass attenuation coefficients, and mass energy–absorption coefficients for ORNL reference newborn bone over the diagnostic energy range.

C. Soft and bone TE substitutes for the child/adult (STES and BTES)

In the ORNL model series, a different reference elemental compositions for both soft tissue and homogeneous skeletal tissue are defined for all ages of the model series older than the newborn (1 years, 5 years, 10 years, 15 years, and adult). In other words, only the newborn model is assigned a unique soft tissue and skeletal elemental composition. Consequently, adjustments to filler material proportions used in STES–NB and BTES–NB were made to create more generic TE substitutes for use in phantom construction in this older age range. In the present study, these TE materials are given the acronyms STES and BTES without the newborn (NB) modifier.

D. Lung tissue-equivalent substitute for the newborn/child/adult (LTES)

A lung tissue-equivalent substitute LTES was manufactured to be radiographically equivalent to reference lung tissue as defined by Cristy and Eckerman[4] in the diagnostic energy range. In the ORNL model series, the elemental composition and mass density of the lungs are kept constant across all ages, and thus only one reference material is prescribed. As with all the other tissue-equivalent materials, LTES is manufactured using a base of Araldite GY-6010 and Jeffamine T-403. The proportions used were roughly similar to those originally proposed for lung-tissue substitutes for use in the therapeutic photon energy range by White and colleagues,[7,9] but adjusted in this study for tissue equivalency at diagnostic energies. In addition to the epoxy resin base, filler materials (polyethylene, silicon dioxide, and magnesium oxide) are used to further adjust the mass density, and energy-dependent values of mass attenuation and mass energy-absorption coefficients. Phenolic microspheres are incorporated to reduce the material's mass density. Final adjustments to mass density are accomplished via a foaming process that employs both a foaming agent, DC 1107, and a surfactant, DC 200/50. This procedure is described in detail by White *et al.*[9]

E. Manufacturing process

A manufacturing process similar to that used by White *et al.*[7,9] is employed for these tissue substitutes. The ingredients are weighed and added in a specific order to facilitate proper mixing of the ingredients as they are combined. First, the epoxy resin is measured, followed by the additions of dry ingredients, phenolic microspheres (if used), and finally the hardener. After all ingredients are added, the mixture is manually stirred until all ingredients have all been incorporated, thus forming a doughy mixture. Only at this point is mechanical mixing begun, in order to minimize loss of dry ingredients. Mechanical mixing is performed with an electric drill using a paint agitator attachment. Soft tissue formulations are mixed three times at five minutes each. Between mixings, the material is placed under vacuum for two minutes each time to evacuate trapped air. Bone formulations are not subjected to a vacuum, as air pockets are released more easily from this less viscous mixture. Lung formulations are subjected to the same mixing process as the soft tissue formulations, but without the application of a vacuum, after which surfactant and foaming agents are added. Additional mechanical mixing distributes these agents. The mixture is then poured into release-treated molds and allowed to foam undisturbed until cured. Further details regarding stylized phantom construction are given in Sessions *et al.*[6]

F. Measurement of TE material mass density

The UF tissue-equivalent substitutes were first compared to ORNL reference tissues on the basis of mass density. While radiation interaction coefficients for a mixture are straightforward to calculate, and can be easily adjusted through changes in ingredient amounts within the final mixture, mass densities do not behave as intuitively as do the interaction coefficients. A simple weighted average of component densities cannot be taken due to potential chemical changes that can occur during material curing and mixing; consequently, it was important to independently measure the mass densities of each of the new tissue-equivalent material prior to their use in phantom construction. These quality assurance measurements were performed for all TE materials with densities exceeding that of water ($\rho_{\text{water}}=0.9975$ to 0.9980 g cm^{-3}, depending upon temperature) using the Archimedean principle:

$$\rho_{\text{material}}=\frac{m}{B}\times\rho_{\text{water}}, \tag{1}$$

where m is the dry mass of the material whose density is being measured, and B is the buoyancy of that material in water (given as the difference in the material's dry mass, m, and the mass of displaced water with the material submerged). The density of LTES, being less than any readily available liquid, was determined in the following manner. A batch of LTES was allowed to cure in a graduated container. While the LTES took the exact shape of that container, the top of the material pour was slightly convex. Water was poured until it just covered the top of the material, and that volume of water was measured in a graduated cylinder and subtracted from the container's volume. The mass of the container was then subtracted from that of the LTES material, and divided by the measured LTES volume to calculate its mass density.

G. Comparison of radiation interaction coefficients

The UF tissue-equivalent substitutes were first compared to their corresponding values for the ORNL reference tissues in terms of both μ/ρ and μ_{en}/ρ as given by the following expressions:

$$\left(\frac{\mu}{\rho}\right)_{\text{TE Material}}=\sum_i w_i\left(\frac{\mu}{\rho}\right)_i, \tag{2}$$

$$\left(\frac{\mu_{\text{en}}}{\rho}\right)_{\text{TE Material}}=\sum_i w_i\left(\frac{\mu_{\text{en}}}{\rho}\right)_i, \tag{3}$$

where w_i is the mass fraction of element i in the TE substitute or ORNL reference tissue. Elemental values of both $(\mu/\rho)_i$ and $(\mu_{\text{en}}/\rho)_i$ were taken from Hubbell and Seltzer[10] and Seltzer,[11] respectively. As discussed in Attix,[12] the weighting factors in Eq. (2) are more properly expressed as $(1-g_i)w_i$, where g_i is the radiation yield fraction for element i in the TE material. Nevertheless, values of g_i are essentially zero in the photon energy range of interest in this study (<150 keV) for all elements considered.

It is also useful to compare the various UF tissue substitutes with existing TE materials in terms of their interaction coefficients over the diagnostic energy range. Several existing tissue substitutes were selected for comparison, including acrylic (also commonly referred to as Plexiglass, Lucite, and PMMA), aluminum, air, MS11, IB1, SB5, and LN 10/75. The latter four materials represent those substitutes developed by White *et al.*[7,9] that are epoxy resin based, and for this reason were selected for comparison to the UF system of materials. MS11 is a muscle-equivalent material. IB1 is constructed to represent an average mixture of osseous bone trabeculae and red marrow defining the interior spongiosa of cancellous bone (22.4% osseous tissue to 77.6% soft tissue).[7] SB5 is a cortical-bone equivalent material, while LN 10/75 is a lung-equivalent material. Polystyrene (soft tissue equivalent) was not considered as it is seldom used in diagnostic radiology except in scatter measurements.[13,14] Our calculations also show that it does not match the ORNL reference soft tissues as closely as does acrylic across the energy range of interest (20 to 80 keV). Copper, a bone-tissue equivalent material, was excluded from the comparisons as it never matches ORNL reference bone tissue as closely as does aluminum (20 to 80 keV). Acrylic and aluminum were selected for comparison because (1) they are commonly used in quality assurance measurements performed on diagnostic equipment, including the construction of patient equivalent phantoms (PEP);[15,16] (2) they are both frequently used in phantom construction for computed and digital radiography;[17–20] and (3) acrylic is the standard material used for QA measurements on CT scanners.[21,22] Air was chosen as it is frequently used in combination with copper, aluminum, and acrylic for construction of diagnostic chest phantoms.[23]

TABLE I. Material compositions of the UF tissue-equivalent substitutes.

Constituent	Material composition (% by mass)				
	STES–NB	BTES–NB	LTES	STES	BTES
Araldite GY6010	50.7	44.6	49.4	51.8	36.4
Jeffamine T-403	20.3	17.9	19.8	20.7	14.6
Polyethylene	8.0		8.0	8.0	
Magnesium oxide	15.5		15.5	15.5	
Silicon dioxide	2.0	15.0	2.0	0.5	25.5
Phenolic microspheres	3.5		3.5	3.5	
Calcium carbonate		19.5			23.5
Polyvinyl chloride		3.0			
DC 1107[a]			0.8		
DC 200/50[a]			1.0		

[a]DC 1107 and DC 200/50 are a foaming agent and a surfactant, respectively, used to inflate LTES.

H. Calculations of x-ray attenuation and absorbed dose at depth

Additional calculations were performed to examine the tissue equivalency of the UF tissue substitutes in predictions of absorbed dose at depth. Estimates were made of both (1) simple exponential attenuation of the x-ray fluence under a narrow-beam geometry, and (2) the single-collision absorbed dose at a depth $x=4$ cm in the UF tissue substitutes, the other TE materials discussed previously, and the corresponding ORNL reference tissues. Expressions for the percent transmission and single-collision point dose at depth are, respectively, given as

$$\frac{\Phi_x}{\Phi_0}=\sum_{i=1}^{N} f_{E_i}\exp-\left[\left(\frac{\mu}{\rho}\right)_{E_i}\rho x\right], \tag{4}$$

$$D_x=\sum_{i=1}^{N}\left(\frac{\mu_{\mathrm{en}}}{\rho}\right)_{E_i}E_i\Phi_{x,E_i}, \tag{5}$$

where Φ_x and Φ_0 are the total fluence of x rays at depth $x=4$ cm and the surface, respectively, E_i is the x-ray energy in the ith energy bin of the x-ray energy spectrum, and f_{Ei}, is the relative spectral weight of the ith energy bin. Values of absorbed dose at depth given by Eq. (5) were based upon a sampling of 10^6 x-ray photons.

In the Neonatal Intensive Care Unit (NICU) at Shands Hospital, radiographs for newborn patients are typically performed with a mobile x-ray unit using computed radiography (CR) technology. For this comparison, x-ray energy spectra were generated using the tungsten anode spectral model TASMIP developed by Boone and Siebert.[24] TASMIP requires three parameters to generate energy spectra: the peak tube potential (kVp), the voltage ripple, and any added filtration. A fixed amount of inherent filtration is assumed in TASMIP if the requested filtration is entered as zero. For the present study, a tube potential of 66 kVp was selected based upon the total mass of the ORNL newborn model and patient mass-dependent technique factors developed in the Department of Radiology for imaging newborn patients. Measurements of the half-value layer (HVL) and voltage ripple at a tube potential of 66 kVp were made on a General Electric model 46-125686G8 x-ray unit commonly used for pediatric Shands NICU studies. The measured first half value layer was 2.33 mm Al, and the measured voltage ripple was 25.6%. Values of added filtration were then evaluated iteratively in a series of Monte Carlo simulations of filtered x-ray fields until the predicted value of HVL matched the measured HVL at 66 kVp. Further experimental details are given in Staton *et al.*[25]

III. RESULTS AND DISCUSSION

A. Comparisons of UF tissue substitutes to reference tissue compositions

The final material compositions of each of the five tissue-equivalent substitutes developed in this study are given in Table I. Corresponding values of the elemental compositions and mass densities of the newborn tissue substitutes (STES–NB, BTES–NB, LTES) are given in Table II along with those of the reference tissues for the ORNL newborn model.[4] At the bottom of Table II, two values of effective atomic number are given as (1) Z_{eff}, defined as a mass-weighted average of the elemental atomic numbers, and $Z_{\mathrm{eff}}^{\mathrm{PE}}$ defined in Attix[12] and in Johns and Cunningham[26] as a more representative quantity for photoelectric absorption. During the development of the tissue substitutes, it was noted that Z_{eff} and $Z_{\mathrm{eff}}^{\mathrm{PE}}$ were good predictors of how well the TE materials' mass attenuation coefficients and mass-energy absorption coefficients, respectively, would match those of the ORNL reference tissues. Table III gives the corresponding values of elemental composition and mass density for the TE substitutes for use in construction of dosimetry phantoms at older patient ages (1 year through the adult). Again, the reference tissues listed in Table III are those used in the ORNL model series, exclusive of the newborn. Targeted mass densities were closely matched for all five TE substitutes.

Figure 1 shows the ratio of μ/ρ (MAC, mass attenuation coefficient) for the various newborn TE substitutes to the corresponding values for the ORNL reference tissues at photon energies from 10 to 150 keV. Values of μ/ρ are noted to

TABLE II. Elemental composition and effective atomic numbers for both the UF newborn tissue-equivalent substitutes and their corresponding reference tissue compositions given for the ORNL newborn model.[a]

	Elemental composition (% by mass)					
Element	STES–NB	Reference soft tissue	BTES–NB	Reference bone tissue	LTES	Reference lung tissue
H	7.0	10.625	5.1	7.995	7.0	10.134
C	58.1	14.964	46.2	9.708	57.4	10.238
N	2.1	1.681	1.9	2.712	2.1	2.866
O	22.3	71.830	30.2	66.811	22.4	75.752
Na		0.075		0.314		0.184
Mg	9.4	0.019		0.143	9.3	0.007
Si	1.0		7.0		1.7	0.006
P		0.179		3.712		0.080
S		0.240		0.314		0.225
Cl	0.1	0.079	1.8	0.140	0.1	0.266
K		0.301		0.148		0.194
Ca		0.003	7.8	7.995		0.009
Fe		0.004		0.008		0.037
Zn						0.001
Rb						0.001
Density	1.04 g/cm^3	1.04 g/cm^3	1.22 g/cm^3	1.22 g/cm^3	0.30 g/cm^3	0.296 g/cm^3
Z_{eff}	6.77	7.02	8.22	8.51	6.83	7.14
Z_{eff}^{PE}	7.65	7.55	10.95	10.84	7.77	7.69

[a]Notes: $Z_{eff}=\Sigma_i w_i Z_i$ and $Z_{eff}^{PE}=\sqrt[3.5]{\Sigma_i a_i Z_i^{3.5}}$ and $a_i=[(w_i Z_i/A_i)/\Sigma_i(w_i Z_i/A_i)]$, where w_i, Z_i, and A_i are the mass fraction, atomic number, and mass number, respectively, of element i.

differ by −0.8% (15 keV) to −3.3% (110–150 keV) of their reference values across this energy range for STES–NB, by −0.1% (20 keV) to −2.6% (140–150 keV) for BTES–NB, and by −0.3% (15 keV) to −2.9% (120–150 keV) for LTES. It can be seen that all μ/ρ values underestimate their respective reference values. This is due to the fact that more emphasis was placed on first matching the mass density and mass energy-absorption coefficients of the tissue substitutes

TABLE III. Elemental composition and effective atomic numbers for the UF tissue-equivalent substitutes needed for phantom construction at ages of 1 year and older. Reference tissue compositions are taken from the ORNL model series at similar ages.[a]

	Elemental composition (% by mass)					
Element	STES	Reference soft tissue	BTES	Reference bone tissue	LTES	Reference lung tissue
H	7.2	10.454	4.0	7.337	7.0	10.134
C	59.2	22.663	37.8	25.475	57.4	10.238
N	2.2	2.490	1.5	3.057	2.1	2.866
O	21.8	63.525	35.3	47.893	22.4	75.752
F				0.025		
Na		0.112		0.326		0.184
Mg	9.3	0.013		0.112	9.3	0.007
Si	0.2	0.030	11.9	0.002	1.7	0.006
P		0.134		5.095		0.080
S		0.204		0.173		0.225
Cl	0.1	0.133	0.1	0.143	0.1	0.266
K		0.208		0.153		0.194
Ca		0.024	9.4	10.190		0.009
Fe		0.005		0.008		0.037
Zn		0.003		0.005		0.001
Rb		0.001		0.002		0.001
Zr		0.001				
Sr				0.003		
Pb				0.001		
Density	1.04 g/cm^3	1.04 g/cm^3	1.40 g/cm^3	1.4 g/cm^3	0.30 g/cm^3	0.296 g/cm^3
Z_{eff}	6.69	6.86	8.80	8.59	6.83	7.14
Z_{eff}^{PE}	7.53	7.43	11.48	11.36	7.77	7.69

[a]Notes: $Z_{eff}=\Sigma_i w_i Z_i$ and $Z_{eff}^{PE}=\sqrt[3.5]{\Sigma_i a_i Z_i^{3.5}}$ and $a_i=[(w_i Z_i/A_i)/\Sigma_i(w_i Z_i/A_i)]$, where w_i, Z_i, and A_i are the mass fraction, atomic number, and mass number, respectively, of element i.

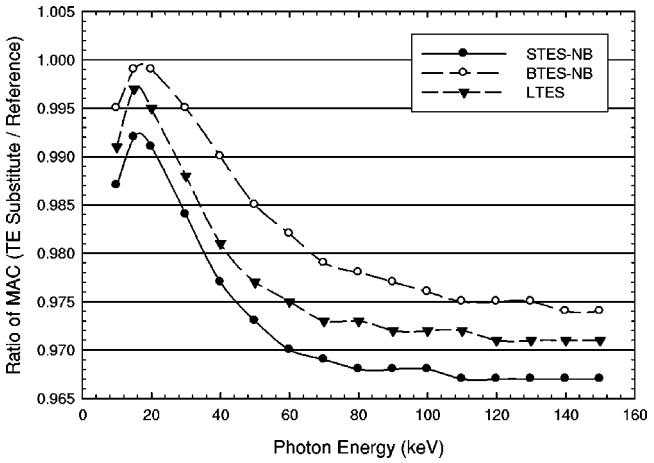

FIG. 1. Ratios of mass attenuation coefficients (MAC or μ/ρ) for the STES–NB, BTES–NB, and LTES tissue substitutes to their corresponding reference values (ORNL newborn model) as a function of photon energy.

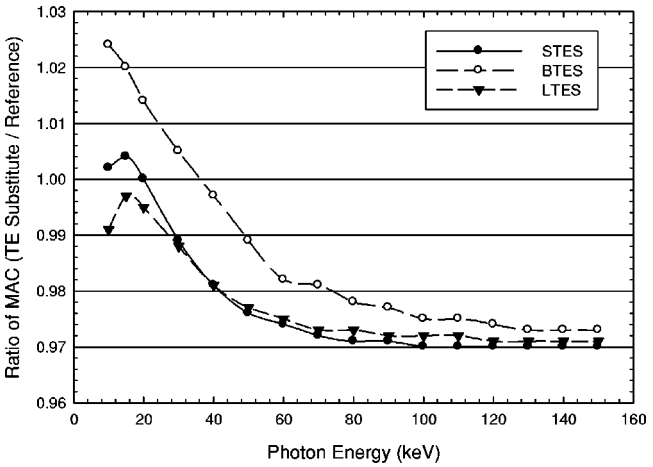

FIG. 3. Ratios of mass attenuation coefficients (MAC) for the STES, BTES, and LTES tissue substitutes to their corresponding reference values (ORNL child/adult models) as a function of photon energy.

to those of the corresponding reference tissues. Corresponding ratios of μ_{en}/ρ (MEAC, mass energy-absorption coefficient) are given in Fig. 2 for these same materials. Values of μ_{en}/ρ range from +1.0% (30 keV) to −3.2% (150 keV) of their reference values across this energy range for STES–NB, from +0.8% (40 keV) to −2.2% (150 keV) for BTES–NB, and from +1.7% (30 keV) to −2.7% (140–150 keV) for LTES. In the energy 20–80 keV, values of μ_{en}/ρ for the three newborn tissue substitutes vary less than ±2% from their reference values. At higher energies (80–140 keV), values of μ_{en}/ρ underestimate their reference values from −1% (BTES–NB) to −3% (STES–NB).

Figure 3 plots the ratio of μ/ρ for STES, BTES, and LTES to their corresponding values for the ORNL reference tissues over the energy range of 10 to 150 keV. Values of μ/ρ for STES are noted to vary from +1.4% (15 keV) to −3.0% (100–150 keV) of their reference values for STES, from +2.4% (10 keV) to −2.6% (130–150 keV) for BTES, and from −0.3% (15 keV) to −2.9% (120–150 keV) for LTES. Corresponding ratios of μ_{en}/ρ for these same materials are given in Fig. 4. Values of μ_{en}/ρ for STES range from +2.0% (30 keV) to −2.9% (150 keV) of their reference values, from +2.9% (10 keV) to −2.5% (150 keV) for BTES, and from +1.7% (30 keV) to −2.7% (140–150 keV) for LTES. In the primary energy range of interest in diagnostic imaging (20 to 80 keV), values of μ_{en}/ρ for the tissue substitutes needed for phantom construction at these older ages vary less than ±2% of the ORNL reference values.

B. Comparison of UF tissue substitutes to other TE materials

Figure 5 plots the ratio of both μ/ρ and μ_{en}/ρ for STES–NB and acrylic to the corresponding ORNL newborn reference tissues[4] as a function of photon energy from 10 to 150 keV. STES–NB is not compared to MS11 because the tissue substitutes developed by White *et al.* were not designed to simulate newborn tissues.[7] Acrylic is shown to approach the tissue equivalency of STES–NB only at energies

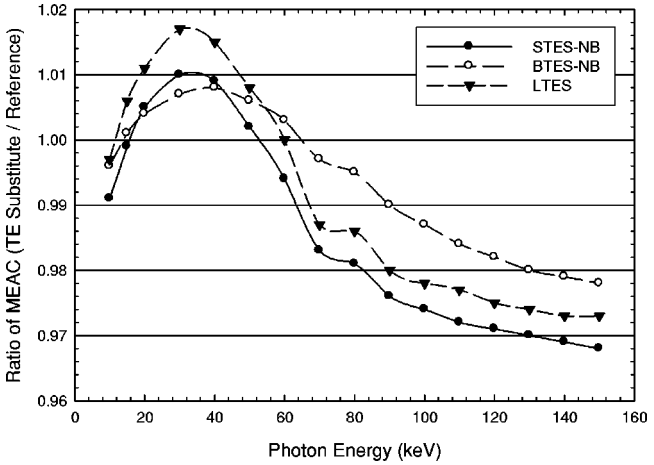

FIG. 2. Ratios of mass energy-absorption coefficients (MEAC or μ_{en}/ρ) for the STES–NB, BTES–NB, and LTES tissue substitutes to their corresponding reference values (ORNL newborn model) as a function of photon energy.

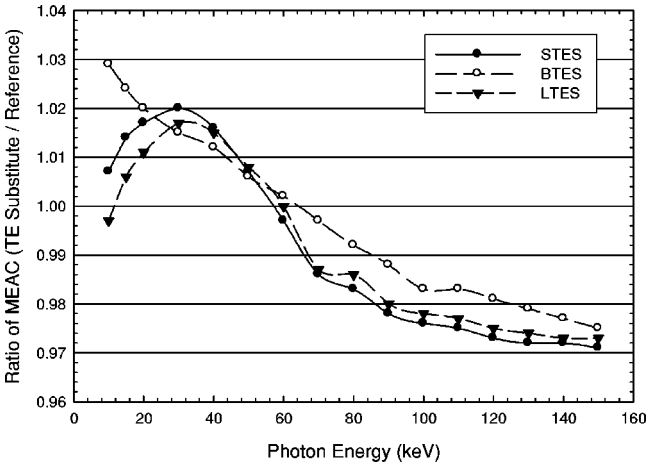

FIG. 4. Ratios of mass energy-absorption coefficients (MEAC) for the STES, BTES, and LTES tissue substitutes to their corresponding reference values (ORNL child/adult models) as a function of photon energy.

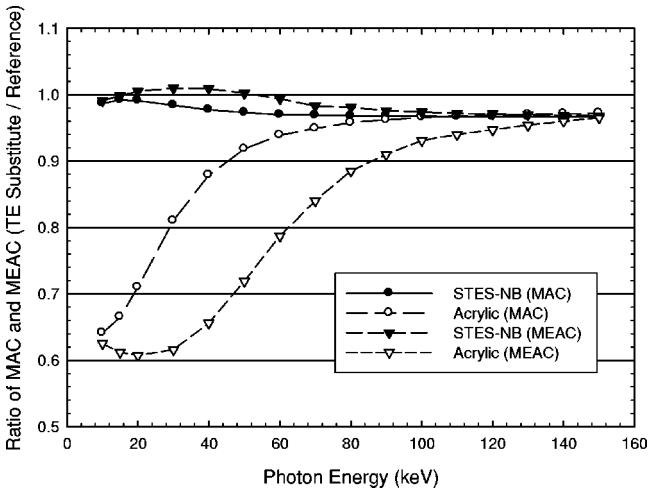

FIG. 5. Ratios of both μ/ρ and μ_{en}/ρ for STES–NB and acrylic to their corresponding reference values (ORNL newborn model) as a function of photon energy.

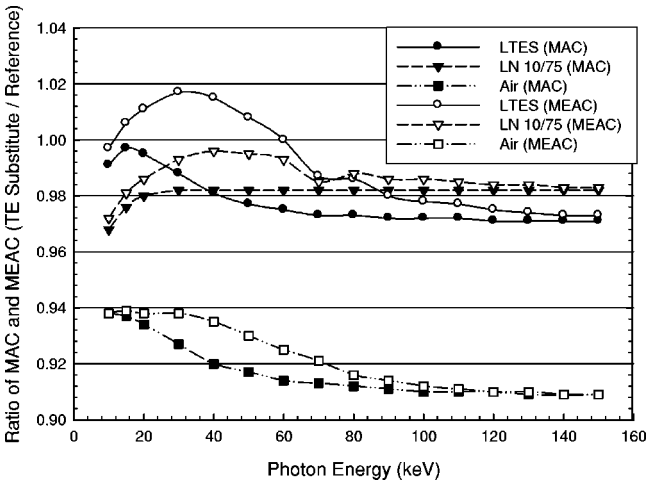

FIG. 7. Ratios of both μ/ρ and μ_{en}/ρ for LTES, LN10/75, and air to their corresponding reference values (ORNL newborn and child/adult models) as a function of photon energy.

exceeding 80 keV in terms of μ/ρ and at energies exceeding 130–140 keV in terms of μ_{en}/ρ. Figure 6 gives a similar comparison between BTES–NB and aluminum over the same energy range. Comparable conclusions are drawn in that aluminum approaches the tissue equivalency of BTES–NB only at energies exceeding 80 and 130–140 keV in terms of μ/ρ and μ_{en}/ρ, respectively.

Figure 7 shows data demonstrating the tissue equivalency of LTES in comparison both to White's LN 10/75 lung substitute[9] and to air. Air is shown to have interaction coefficients that are from −6% to −10% of the ORNL reference lung tissue. At the higher energies (>80 keV), the agreement with reference lung tissue for μ_{en}/ρ is slightly better for LN 10/75 (ratios of 0.988–0.983) than for LTES (ratios of 0.985–0.973). Values of μ_{en}/ρ for LTES, however, begin to exceed those ORNL reference lung tissue at lower energies (<60 keV), and thus a weighting of μ_{en}/ρ for LTES over a typical diagnostic energy spectrum would potentially show improved lung tissue equivalency than seen for LN 10/75 in construction of either newborn or child/adult dosimetry phantoms.

In Fig. 8 we compare the tissue equivalency of STES both with White's muscle-equivalent substitute MS11 and with acrylic. While all materials show essentially equivalent agreement with interaction coefficients for reference child/adult soft tissue at energies exceeding ~100 keV, acrylic is shown to continually underestimate values of μ/ρ and μ_{en}/ρ at lower and lower photon energies. Values of μ/ρ for both STES and MS11, relative to the ORNL reference soft tissue for the child/adult, are reasonably comparable at all photon energies. However, the agreement in values of μ_{en}/ρ is improved for STES over MS11 at energies below 100 keV.

A final series of comparisons for bone-equivalent materials are given in Figs. 9 and 10 for μ/ρ and μ_{en}/ρ, respectively. In addition to BTES, comparisons to ORNL reference

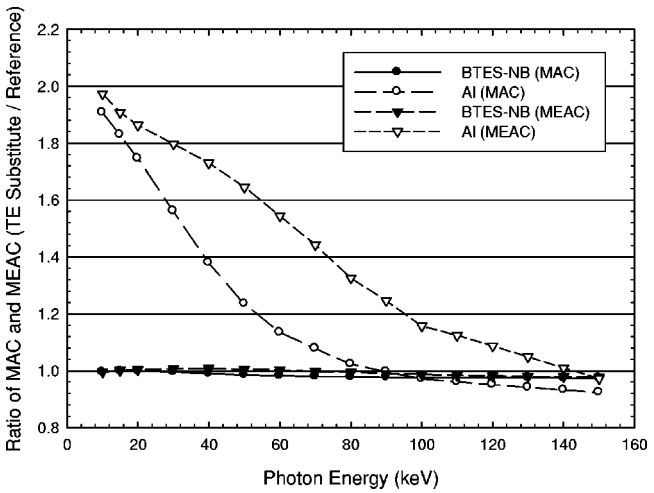

FIG. 6. Ratios of both μ/ρ and μ_{en}/ρ for BTES–NB and aluminum to their corresponding reference values (ORNL newborn model) as a function of photon energy.

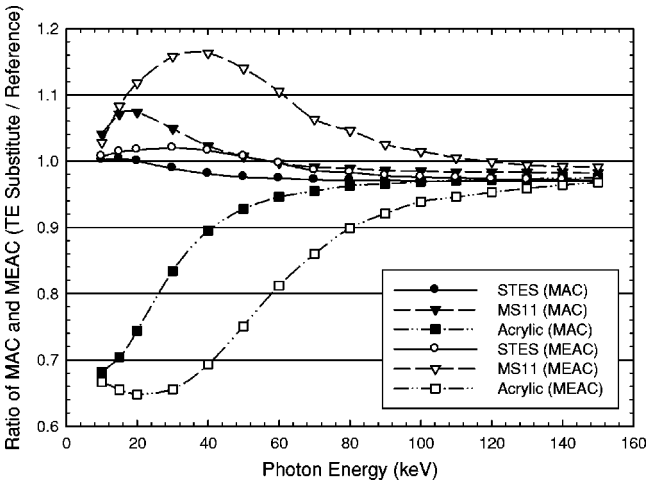

FIG. 8. Ratios of both μ/ρ and μ_{en}/ρ for STES, MS11, and acrylic to their corresponding reference values (ORNL child/adult models) as a function of photon energy.

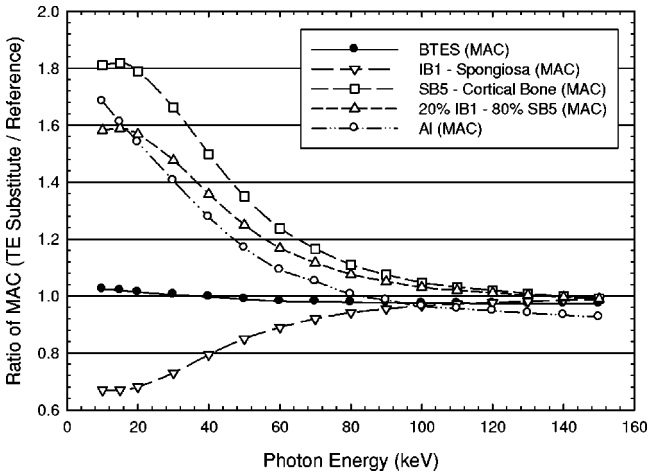

FIG. 9. Ratios of μ/ρ for BTES, IB1, SB5, weighted combination of IB1 and SB5, and aluminum to their corresponding reference values (ORNL child/adult models) as a function of photon energy.

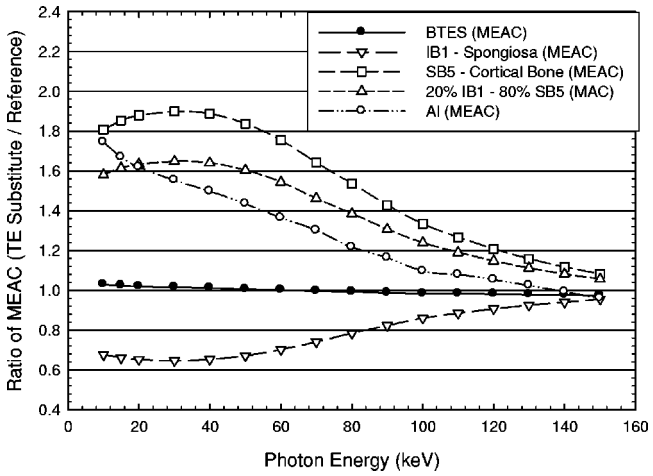

FIG. 10. Ratios of μ_{en}/ρ for BTES, IB1, SB5, weighted combination of IB1 and SB5, and aluminum to their corresponding reference values (ORNL child/adult models) as a function of photon energy.

bone tissue (child/adult) are given for White's spongiosa substitute (IB1), White's cortical bone substitute (SB5), and aluminum. Another set of plots is given in which the curves for IB1 and SB5 are weighted in proportions representative of cortical and trabecular bone in Reference Man.[27,28] As shown in Fig. 9, agreement with reference bone tissue in values of μ/ρ are shown to be comparable for all materials at photon energies of 100 keV and higher. The data of Fig. 10 indicate that similar agreement in terms of reference values of μ_{en}/ρ are not seen until the photon energies exceed perhaps 140 keV. Values of both μ/ρ and μ_{en}/ρ for BTES are shown to closely match (within a few percent) those for the ORNL reference bone tissue for the child/adult across the full energy range of interest in pediatric radiology.

C. Calculations of x-ray attenuation and absorbed dose at depth

Table IV gives results for both x-ray attenuation and point absorbed dose at 4 cm depth for each of the five reference tissues and other TE materials discussed previously. Percent differences are shown for each value relative to those determined in the corresponding ORNL reference tissues. Percent

TABLE IV. Results for calculations of narrow-beam photon transmission (66 kVp energy spectrum) through 4 cm of tissue-equivalent material and the resulting single-collision absorbed dose delivered at that depth. The absorbed dose is calculated based upon an emission of 10^6 x-ray photons.

Tissue-equivalent material	Percent transmission (%)	% Difference from reference tissue	Absorbed dose at 4 cm depth (μGy)	% Difference from reference tissue
Soft tissue				
STES–NB	27.7	+2.6%	0.145	+3.6%
Acrylic	27.8	+3.0%	0.098	−30.0%
Reference soft tissue (newborn)	27.0		0.140	
STES	28.1	+1.4%	0.143	+3.6%
MS11	28.4	+2.5%	0.161	+16.7%
Reference soft tissue (child/adult)	27.7		0.138	
Bone tissue				
BTES–NB	10.8	+1.9%	0.130	+3.2%
Aluminum	0.6	−94.3%	0.008	−93.7%
Reference bone tissue (newborn)	10.6		0.126	
BTES	6.6	−5.7%	0.086	−4.4%
IB1	15.0	+114%	0.347	+285%
SB5	1.3	−81.4%	0.025	−72.2%
20% IB1+80% SB5	2.1	−70.0%	0.037	−58.9%
Reference bone tissue (child/adult)	7.0		0.090	
Lung tissue				
LTES	67.0	+0.1%	0.420	+1.2%
Air	99.8	+49.2%	0.631	+52.0%
LN 75/100	66.4	−0.7%	0.408	−1.7%
Reference lung tissue	66.9		0.415	

differences in absorbed dose are shown to be +3.6% for both the newborn and child/adult soft tissue-equivalent substitutes STES–NB and STES. Similarly, dosimetry errors are noted to be +3.2% of reference values for newborn skeletal tissue, −4.4% for child/adult skeletal tissue, and +1.2% for lung tissue (both newborn and child/adult). Of the materials developed by White *et al.*,[7–9] only the lung equivalent material LN 75/100 shows a comparable level of agreement to the ORNL reference tissues (percent difference of −1.7%).

IV. CONCLUSIONS

Five tissue-equivalent substitutes are presented for use in the construction of tomographic, or image-based, phantoms for organ dose assessment in pediatric radiology.[3,6] STES–NB, BTES–NB, and LTES are described and characterized as materials radiographically mimicking the soft tissue, skeletal tissues, and lung tissues of the newborn patient. In their development, the elemental compositions given by Cristy and Eckerman[4] for the ORNL newborn stylized computational model are used as a reference standard for their manufacture. In the ORNL model series, no changes are noted for lung tissues between the newborn and the models of older individuals (1 year old through adult), and thus only a single lung-equivalent material has been developed. Additionally, STES and BTES are described and characterized as matching the soft tissue and skeletal tissues of the child (1 year to 15 year) and adult.

Values of μ/ρ for the newborn tissue substitutes STES–NB, BTES–NB, and LTES are noted to underestimate their values for the reference tissues by approximately 3.3%, 2.5%, and 2.9%, respectively, at photon energies exceeding 80–90 keV (see Fig. 1). As the photon energy decreases, the agreement improves to within 1% at 15–20 keV. Values of μ_{en}/ρ for these same materials are shown to overestimate their values for reference tissues between 20 and 60–70 keV by 1–2 %, and then underestimate their values for reference tissues at higher energies (see Fig. 2). At 120 keV, for example, STES–NB, BTES–NB, and LTES are noted to underestimate values of μ_{en}/ρ for reference tissues by 2.9%, 2.5%, and 1.8%, respectively. As shown in Figs. 3 and 4, comparable comparisons of both μ/ρ and μ_{en}/ρ to ORNL reference tissues are noted for the tissue substitutes STES and BTES. Estimates of point absorbed dose at 4 cm depth are given in Table IV which indicate dosimetry errors from reference tissues of between 3.2% to 4.4% for STES–NB, STES, and BTES–NB and 1.2% for LTES. The good agreement seen for STES–NB, BTES–NB, and LTES in their comparisons to ORNL reference newborn tissues allows us to proceed with the construction of physical tomographic model of the newborn following the CT image segmentation previously described by Nipper *et al.*[3]

ACKNOWLEDGMENTS

This work was supported by Grant No. RO1 HD38932-02 with the National Institute for Child and Health Development (NICHD) and Grant No. RO1 EB 00267-03 with the National Institute for Biomedical Imaging and Bioengineering (NIBIB) with the University of Florida.

[a]Author to whom correspondence should be addressed; electronic mail: wbolch@ufl.edu

[1] R. Kienböck, "On the quantimetric method," Arch Roentgen Ray **11**, 17 (1906).
[2] ICRU, *Tissue Substitutes in Radiation Dosimetry and Measurement*, ICRU Report 44 (International Commission on Radiation Units and Measurements, Bethesda, MD, 1989).
[3] J. Nipper, J. Williams, and W. Bolch, "Creation of two tomographic voxel models of pediatric patients in the first year of life," Phys. Med. Biol. **47**, 3143–3164 (2002).
[4] M. Cristy and K. F. Eckerman, *Specific Absorbed Fractions of Energy at Various Ages from Internal Photon Sources*, ORNL/TM-8381/Volumes I–VII (Oak Ridge National Laboratory, Oak Ridge, 1987).
[5] ICRU, *Photon, Electron, Proton and Neutron Interaction Data for Body Tissues*, Report 46 (International Commission on Radiation Units and Measurements, Bethesda, MD, 1992).
[6] J. Sessions, J. Roshau, M. Tressler, D. Hintenlang, M. Arreola, J. Williams, and W. Bolch, "Comparisons of point and average organ dose within an anthropomorphic physical phantom and a computational model of the newborn patient," Med. Phys. **29**, 1080–1089 (2002).
[7] D. R. White, R. J. Martin, and R. Darlison, "Epoxy resin based tissue substitutes," Br. J. Radiol. **50**, 814–821 (1977).
[8] D. R. White, "The formulation of tissue substitute materials using basic interaction data," Phys. Med. Biol. **22**, 889–899 (1977).
[9] D. R. White, C. Constantinou, and R. J. Martin, "Foamed epoxy resin-based lung substitutes," Br. J. Radiol. **59**, 787–790 (1986).
[10] J. Hubbell and S. Seltzer, *Tables of X-ray Attenuation Coefficients 1 keV to 20 MeV for Elements Z=1 to 92 and Additional Substances of Dosimetric Interest*, Report NISTIR 5632 (National Institute of Standards and Technology, Gaithersburg, MD, 1995).
[11] S. M. Seltzer, "Calculation of photon mass energy-transfer and mass energy-absorption coefficients," Radiat. Res. **136**, 147–170 (1993).
[12] F. H. Attix, *Introduction to Radiological Physics and Radiation Dosimetry* (Wiley, New York, NY, 1986).
[13] C. E. Dick, C. G. Soares, and J. W. Motz, "X-ray scatter data for diagnostic radiology," Phys. Med. Biol. **23**, 1076–1085 (1978).
[14] J. W. Motz and C. E. Dick, "X-ray scatter background signals in transmission radiography," Med. Phys. **2**, 259–267 (1975).
[15] K. A. Fetterly and N. J. Hangiandreou, "Effects of x-ray spectra on the DQE of a computed radiography system," Med. Phys. **28**, 241–249 (2001).
[16] B. J. Conway, J. E. Duff, T. R. Fewell, R. J. Jennings, L. N. Rothenberg, and R. C. Fleischman, "A patient-equivalent attenuation phantom for estimating exposures from automatic exposure controlled x-ray examinations of the abdomen and lumbo-sacral spine," Med. Phys. **17**, 448–453 (1990).
[17] B. J. Conway, J. E. Duff, T. R. Fewell, R. J. Jennings, L. N. Rothenberg, and R. C. Fleischman, "A patient-equivalent attenuation phantom for estimating patient exposures from automatic exposure controlled x-ray examinations of the abdomen and lumbo-sacral spine," Med. Phys. **17**, 448–453 (1990).
[18] E. Mah, E. Samei, and D. J. Peck, "Evaluation of a quality control phantom for digital chest radiography," J. Appl. Clin. Med. Phys. **2**, 90–101 (2001).
[19] H. G. Chotas, C. E. Floyd, Jr., G. A. Johnson, and C. E. Ravin, "Quality control phantom for digital chest radiography," Radiology **202**, 111–116 (1997).
[20] H. G. Chotas, R. L. Van Metter, G. A. Johnson, and C. E. Ravin, "Small object contrast in AMBER and conventional chest radiography," Radiology **180**, 853–859 (1991).
[21] R. J. Scheck, E. M. Coppenrath, M. W. Kellner, K. J. Lehmann, C. Rock, J. Rieger, L. Rothmeier, F. Schweden, A. A. Bauml, and K. Hahn, "Radiation dose and image quality in spiral computed tomography: multicenter evaluation at six institutions," Br. J. Radiol. **71**, 734–744 (1998).
[22] C. H. McCollough and F. E. Zink, "Performance evaluation of a multislice CT system," Med. Phys. **26**, 2223–2230 (1999).
[23] J. Vassileva, "A phantom for dose-image quality optimization in chest radiography," Br. J. Radiol. **75**, 837–842 (2002).

[24] J. M. Boone and J. A. Seibert, ''An accurate method for computer-generating tungsten anode x-ray spectra from 30 to 140 kV,'' Med. Phys. **24**, 1661–1670 (1997).
[25] R. Staton, F. Pazik, J. Nipper, J. Williams, and W. Bolch, ''A comparison of newborn stylized and tomographic models for dose assessment in pediatric radiology,'' Phys. Med. Biol. **48**, 805–820 (2003).
[26] H. E. Johns and J. R. Cunningham, *The Physics of Radiology*, 4th ed. (Charles C. Thomas Publishers, Springfield, IL, 1983).
[27] ICRP, *Limits for Intakes of Radionuclides by Workers*, ICRP Publication 30 (International Commission on Radiological Protection, Oxford, UK, 1979).
[28] ICRP, *Report on the Task Group on Reference Man*, ICRP Publication 23 (International Commission on Radiological Protection, Oxford, UK, 1975).